Diffractive lenses recorded in absorbent photopolymers

R. Fernández,[1] S. Gallego,[1,2,*] A. Márquez,[1,2] J. Francés,[1,2] V. Navarro-Fuster,[3] and I. Pascual[1,3]

[1]*Instituto Universitario de Física Aplicada a las Ciencias y las Tecnologías, Universidad de Alicante. Apartado 99, 03080 Alicante, Spain*

[2]*Departamento de Física, Ingeniería de Sistemas y Teoría de la Señal. Universidad de Alicante. Apartado 99. E03080 Alicante, Spain*

[3]*Departamento de Óptica, Farmacología y Anatomía. Universidad de Alicante. Apartado 99. E03080 Alicante, Spain*

[*]*sergi.gallego@ua.es*

Abstract: Photopolymers can be appealing materials for diffractive optical elements fabrication. In this paper, we present the recording of diffractive lenses in PVA/AA (Polyvinyl alcohol acrylamide) based photopolymers using a liquid crystal device as a master. In addition, we study the viability of using a diffusion model to simulate the lens formation in the material and to study the influence of the different parameters that govern the diffractive formation in photopolymers. Once we control the influence of each parameter, we can fit an optimum recording schedule to record each different diffractive optical element with the optimum focalization power.

OCIS codes: (050.0050) Diffraction and gratings; (050.1965) Diffractive lenses; (160.5335) Photosensitive materials.

References and links

1. M. D. Lechner, "Photopolymers for optical memories and waveguides," Electron. Prop. Polym. Relat. Compd. **63**, 301–308 (1985).
2. H. J. Coufal, D. Psaltis, and G. T. Sincerbox, eds., *Holographic Data Storage* (Springer–Verlag, 2000).
3. E. Hata, K. Mitsube, K. Momose, and Y. Tomita, "Holographic nanoparticle-polymer composites based on step-growth thiol-ene photopolymerization," Opt. Mater. Express **1**(2), 207–222 (2011).
4. A. Olivares-Pérez, S. Toxqui-López, and A. L. Padilla-Velasco, "Nopal Cactus (Opuntia Ficus-Indica) as a Holographic Material," Materials (Basel) **5**(12), 2383–2402 (2012).
5. P. Cheben and M.-L. Calvo, "A Photopolymerizable Glass with Diffraction Efficiency Near 100% for Holographic Storage," Appl. Phys. Lett. **78**, 1490–1492 (2001).
6. M. Miki, R. Ohira, and Y. Tomita, "Optical properties of electrically tunable two-dimensional photonic lattice structures formed in a holographic polymer-dispersed liquid crystal film: analysis and experiment," Materials (Basel) **7**(5), 3677–3698 (2014).
7. M. Infusino, A. De Luca, V. Barna, R. Caputo, and C. Umeton, "Periodic and aperiodic liquid crystal-polymer composite structures realized via spatial light modulator direct holography," Opt. Express **20**(21), 23138–23143 (2012).
8. C. E. Close, M. R. Gleeson, and J. T. Sheridan, "Monomer Diffusion Rates in Photopolymer Material: Part I: Low Spatial Frequency Holographic Gratings," J. Opt. Soc. Am. B **28**(4), 658–666 (2011).
9. R. Fernández, S. Gallego, J. Francés, I. Pascual, and A. Beléndez, "Characterization and comparison of different photopolymers for low spatial frequency recording,"," Opt. Mater. **44**, 18–24 (2015).
10. J. Zhu, G. Wang, Y. Hao, B. Xie, and A. Y. S. Cheng, "Highly sensitive and spatially resolved polyvinyl alcohol/acrylamide photopolymer for real-time holographic applications," Opt. Express **18**(17), 18106–18112 (2010).
11. E. Tolstik, O. Romanov, V. Matusevich, A. Tolstik, and R. Kowarschik, "Formation of self-trapping waveguides in bulk PMMA media doped with Phenanthrenequinone," Opt. Express **22**(3), 3228–3233 (2014).
12. E. Leite, I. Naydenova, S. Mintova, L. Leclercq, and V. Toal, "Photopolymerizable nanocomposites for holographic recording and sensor application," Appl. Opt. **49**(19), 3652–3660 (2010).
13. S. Gallego, A. Márquez, M. Ortuño, J. Francés, I. Pascual, and A. Beléndez, "Relief diffracted elements recorded on absorbent photopolymers," Opt. Express **20**(10), 11218–11231 (2012).
14. A. C. Urness, K. Anderson, C. Ye, W. L. Wilson, and R. R. McLeod, "Arbitrary GRIN component fabrication in optically driven diffusive photopolymers," Opt. Express **23**(1), 264–273 (2015).

#251920 Received 14 Oct 2015; revised 11 Dec 2015; accepted 17 Dec 2015; published 20 Jan 2016

15. A. K. Kirby, P. J. Hands, and G. D. Love, "Liquid crystal multi-mode lenses and axicons based on electronic phase shift control," Opt. Express **15**(21), 13496–13501 (2007).
16. M. R. Gleeson, J. T. Sheridan, F. K. Bruder, T. Rölle, H. Berneth, M. S. Weiser, and T. Fäcke, "Comparison of a new self developing photopolymer with AA/PVA based photopolymer utilizing the NPDD model," Opt. Express **19**(27), 26325–26342 (2011).
17. T. Babeva, I. Naydenova, D. Mackey, S. Martin, and V. Toal, "Two-way diffusion model for short-exposure holographic grating formation in acrylamide-based photopolymer," J. Opt. Soc. Am. B **27**(2), 197–203 (2010).
18. S. Gallego, R. Fernández, A. Márquez, M. Ortuño, C. Neipp, M. R. Gleeson, J. T. Sheridan, and A. Beléndez, "Two diffusion photopolymer for sharp diffractive optical elements recording," Opt. Lett. **40**(14), 3221–3224 (2015).
19. S. Gallego, A. Márquez, D. Méndez, C. Neipp, M. Ortuño, M. Alvarez, E. Fernandez, and A. Beléndez, "Real-time interferometric characterization of a polyvinyl alcohol based photopolymer at the zero spatial frequency limit," Appl. Opt. **46**(30), 7506–7512 (2007).
20. A. Márquez, S. Gallego, M. Ortuño, E. Fernández, M.L. Álvarez, A. Beléndez; I. Pascual, "Generation of diffractive optical elements onto a photopolymer using a liquid crystal display," Proc. SPIE **7717**, 77170D (2010).
21. F. J. Martínez, A. Márquez, S. Gallego, M. Ortuño, J. Francés, I. Pascual, and A. Beléndez, "Predictive capability of average Stokes polarimetry for simulation of phase multilevel elements onto LCoS devices," Appl. Opt. **54**(6), 1379–1386 (2015).
22. S. Gallego, R. Fernández, A. Márquez, F. J. Martínez, C. Neipp, M. Ortuño, J. Francés, A. Beléndez, and I. Pascua, "Influence of the photopolymer properties in the fabrication of diffractive optical elements," Proc. SPIE, Optics and Photonics for Information Processing VIII, 9216, 9 pag. (2014).
23. S. Gallego, A. Márquez, M. Ortuño, J. Francés, I. Pascual, and A. Beléndez, "Diffractive and interferometric methods to characterize photopolymers with liquid crystal molecules as holographic recording material," J. European Opt. Soc. **7**, 12024 (2012).
24. J. W. Goodman, *Introduction to Fourier Optics* (McGraw-Hill 1987).

1. Introduction

Photopolymers are one of the most versatile and cheapest optical recording materials due to their dynamical chemical composition and the possibility of introducing many new components. Therefore, they have been designed for many different optical applications from waveguides to holographic data storage discs [1–5]. Their initial chemical formulations, used mainly for recording holograms, were slightly modified in order to offer broad possible applications [6,7]. One of them was the fabrication of diffractive optical elements, using two properties: the relief structures formed on the surface and the refractive index modulation distribution. In this sense, some chemical compositions have been analyzed and evaluated the possible effects of the index matching substances and covering architectures [8,9].

One of the most studied photopolymers is the one based on polyvinyl alcohol acrylamide (PVA/AA) [8–12]. This photopolymer was proposed for different applications such as for wave guide [11], aligning liquid crystal molecules, or sensors [12]. Furthermore, some compositions have shown their viability to record simple diffractive elements, like sinusoidal gratings, binary, blazed, diffractive lenses or fork ones [7, 13, 14]. In this work, we propose this type of materials to fabricate more complex diffractive elements: lenses.

For many diffractive optical elements, such as lenses or axicons, a phase depth of 2π is required; this value depends on the refractive index variation and the thickness. Therefore, before the first attempt to record these elements it is important to be sure that the material can achieve this limit. In this sense, we have developed different studies with some photopolymers families [9] to find out the minimum thickness required to obtain this phase depth value for each chemical composition.

Parallel to the development of new photopolymer materials, some investigations were performed involving theoretical models to simulate the recording process and the post evolution of photopolymers [7, 16–18]. Usually these models have been applied to simulate the diffraction gratings formation analyzing different shapes, spatial frequencies, the effects of the addition of a new chemical component and the attenuation of the grating in depth. Recently these models have shown their utility to analyze the formation of 2-D photonic structures [7]. In the present work we validate one of these models to predict the lens

#251920 Received 14 Oct 2015; revised 11 Dec 2015; accepted 17 Dec 2015; published 20 Jan 2016

formation in PVA/AA photopolymers once the material parameters have been determined experimentally using the diffractive and interferometric techniques presented in [19].

In particular, in this paper we focus our attention on the recording of diffractive optical elements using a coverplated photopolymer based material. Due to the use of glycerin as an index matching component, only the refractive index distribution will affect the transmitted light [18]. To support and to optimize our experiments we have used a diffusion model successfully applied for the simulation of very low spatial frequency gratings. The diffractive lenses are projected onto the material using a last generation spatial light modulator based on Liquid a Cristal on Silicon (LCoS) microdisplay working in the amplitude mode.

2. Theoretical diffusion model

We use a coverplated and index matched photopolymer to avoid the influence of the thickness variation on the transmitted light. In order to simulate the material behavior during polymerization we have designed our model to simulate cylindrical lenses as well as spherical ones.

The three dimensional behavior for the cylindrical lenses can be described by 2 spatial dimensions functions due to their symmetry; therefore, we can use the following general Eqs., taking into account that the light is propagating in the Z positive direction:

$$\frac{\partial M(x,z,t)}{\partial t} = \frac{\partial}{\partial z} D_m(t) \frac{\partial M(x,z,t)}{\partial z} + \frac{\partial}{\partial x} D_m(t) \frac{\partial M(x,z,t)}{\partial x} - F_R(x,z,t) M(x,z,t) \quad (1)$$

$$\frac{\partial P(x,z,t)}{\partial t} = F_R(x,z,t) M(x,z,t) \quad (2)$$

where D_m is the monomer diffusion inside the material, F_R is the polymerization rate and M and P are the volume fraction of the monomer and polymer respectively. The initial value of D_m [$D_m(t=0) = D_0$] was measured using diffractive techniques as in [9].

In the spherical lenses case we have to add one dimension (the one related with the 'y' variable), then the differential equations can be written as follows:

$$\begin{aligned} \frac{\partial M(x,y,z,t)}{\partial t} &= \frac{\partial}{\partial z} D_m(t) \frac{\partial M(x,y,z,t)}{\partial z} + \frac{\partial}{\partial y} D_m(t) \frac{\partial M(x,y,z,t)}{\partial y} \\ &+ \frac{\partial}{\partial x} D_m(t) \frac{\partial M(x,y,z,t)}{\partial x} - F_R(x,z,t) M(x,z,t) \end{aligned} \quad (3)$$

$$\frac{\partial P(x,y,z,t)}{\partial t} = F_R(x,y,z,t) M(x,y,z,t) \quad (4)$$

The polymerization rate depends on the reaction kinetics and the recording intensity; this dependence can be described by the above equation:

$$F_R(x,y,z,t) = k_R(x,y,z,t) I(x,y,z,t)^{\gamma} = k_R(x,y,z,t) I(x,y)^{\gamma} e^{-\alpha(t)\gamma z} \quad (5)$$

I is the recording intensity, k_R is the polymerization velocity, which depends on the kinetics of the photochemical reaction [9], γ indicates the relationship between intensity and polymerization rate; α is the coefficient of light attenuation. The initial value of α [$\alpha(t=0) = \alpha_0$] can be obtained if the transmittance and the physical thickness of the layer are known and its variation as a function of the light dose is related to the bleaching process of the material when the dye is consumed. The influence of these parameters of the material: k_R, α and D_0 will be analyzed in the section 4.3 of this work, to simulate how would be recorded diffractive lenses using the proposed method in photopolymers with different properties.

#251920 Received 14 Oct 2015; revised 11 Dec 2015; accepted 17 Dec 2015; published 20 Jan 2016

The recording intensity distribution from the spatial light modulator in the amplitude regime is projected on the material and produces the corresponding phase element. In particular, in the case of the spherical lens with focal f, we need to generate a convergent spherical wave front, where the phase depends on the quadratic value of the distance between the point and the lens centrum, thus we want to obtain at the first attempt can be write as:

$$I(x,y) = \exp\left[j \frac{\pi}{\lambda f}(x^2 + y^2) \right] \tag{6}$$

To obtain this phase distribution we assume a linear response of the recording material concerting an amplitude distribution generated by LCoS into a phase distribution. Therefore Eq. (6) has to be wrapped to 2π value and normalized to the maximum of the intensity, I_0. In this sense for f = 1m when we imaged an amplitude distribution with a maximum intensity in the middle and there are a series of rings of zeros located at:

$$r_m = \sqrt{m(2\lambda f)} \tag{7}$$

where m is a natural number, f is the focal length and λ is the light wavelength. Moreover, we know that the maximum phase shift achieved for photopolymers at these spatial frequencies range is slightly higher than 2π. Therefore, we have to wrap the phase as is depicted in Fig. 1 ; this desired intensity distribution is generated using a LCD.

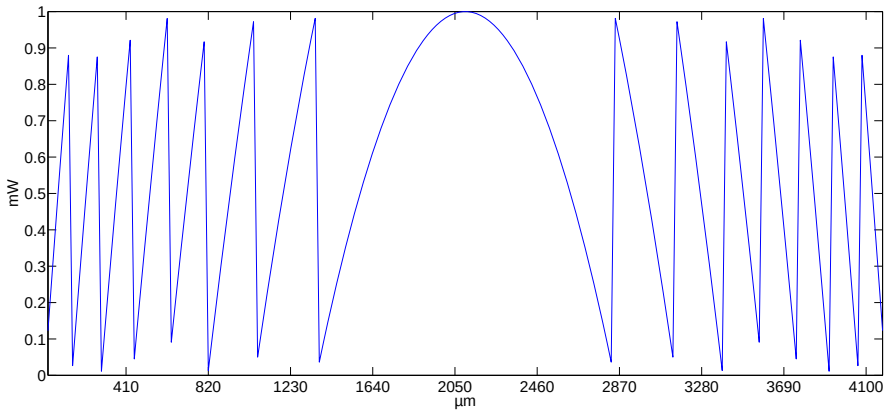

Fig. 1 Theoretical intensity distribution (horizontal cut) projected onto photopolymer for a focal length of 50 cm.

There are different methods to solve these differential equations. In this paper we use the finite-difference method (FDM) to solve a 3-dimensional problem using a rigorous method. Therefore, Eqs. (1) and (2) can be written as:

$$\begin{aligned} M_{i,j,k} &= \frac{\Delta t}{\Delta x^2} D_m(t) M_{i+1,j,k-1} - 2\frac{\Delta t}{\Delta x^2} D_m(t) M_{i,j,k-1} + \frac{\Delta t}{\Delta x^2} D_m(t) M_{i-1,j,k-1} + \frac{\Delta t}{\Delta z^2} D_m(t) M_{i,j+1,k-1} \\ &-2\frac{\Delta t}{\Delta z^2} D_m(t) M_{i,j,k-1} + \frac{\Delta t}{\Delta z^2} D_m(t) M_{i,j-1,k-1} - \Delta t F_{R_{i,j,k-1}} M_{i,j,k1} + M_{i,j,k-1} \end{aligned} \tag{8}$$

$$P_{i,j,k} = P_{i,j,k} + \Delta t \cdot F_{R_{i,j,k-1}} \cdot M_{i,j,k-1} \tag{9}$$

For the spherical lenses, the Eqs. (8) and (9) are the following:

#251920 Received 14 Oct 2015; revised 11 Dec 2015; accepted 17 Dec 2015; published 20 Jan 2016

$$M_{i,l,j,k} = \frac{\Delta t}{\Delta x^2} D_m M_{i+1,l,j,k-1} - 2\frac{\Delta t}{\Delta x^2} D_m(t) M_{i,l,j,k-1} + \frac{\Delta t}{\Delta x^2} D_m(t) M_{i-1,l,j,k-1} +$$
$$\frac{\Delta t}{\Delta y^2} D_m(t) M_{i,l+1,j,k-1} - 2\frac{\Delta t}{\Delta y^2} D_m(t) M_{i,l,j,k-1} + \frac{\Delta t}{\Delta y^2} D_m(t) M_{i,l-1,j,k-1} + \frac{\Delta t}{\Delta z^2} D_m(t) M_{i,l,j+1,k-1} - \quad (10)$$
$$2\frac{\Delta t}{\Delta z^2} D_m(t) M_{i,l,j,k-1} + \frac{\Delta t}{\Delta z^2} D_m(t) M_{i,l,j-1,k-1} = \Delta t F_{R_{i,j,k-1}} M_{i,l,j,k.1} + M_{i,l,j,k-1}$$

$$F_{Ri,l,j,k} = F_{Ri,l,j,k-1} + \Delta t\, F_{Ri,l,j,k-1} M_{i,l,j,k-1} + M_{i,l,j,k-1} \quad (11)$$

In order to guarantee the numerical stability of the Eqs., the increment in the time domain, Δt, must satisfy the stability criterion:

$$\Delta t < \frac{1}{2}\left(\frac{\Delta x^2}{D_m}\right) \quad (12)$$

In this case, we choose $\Delta t = 0.1\ (\Delta x^2/D_m)$

Once we obtain the monomer and polymer concentrations, we can use the refractive index values to obtain the refractive index distribution during the recording process. The refractive index distribution can be measured using Lorenz-Lorenz Eq. as follows:

$$\frac{n^2-1}{n^2+2} = \frac{n_m^2-1}{n_m^2+2} M + \frac{n_p^2-1}{n_p^2+2} P + \frac{n_b^2-1}{n_b^2+2}(1-M_0) \quad (13)$$

Where M0 is the average initial value for the volume fraction of monomer, np is the polymer refractive index, nm is the monomer refractive index, nb is the binder refractive index. The last two parameters can be measured using a refractometer and the value of np can be obtained using the zero spatial frequency technique [19].

3. Experimental set-up

In order to analyze in real time the formation of the phase object in the recording material we use the experimental set-up in Fig. 2. In This setup is both used to register and analyze the diffractive optical lenses. The recording process uses the wavelength 532 nm, and the lenses are calculate to be used with the 633 nm wavelength. The system is designed to measure the performance of the lenses in real-time while the recording process is taking place.

We distinguish two arms: the recording arm, using the wavelength 532 nm provided by a solid-state Verdi laser (Nd-YVO4), and the analyzing arm, using the wavelength 633 nm, where the material presents no absorption, provided by a He-Ne laser. In the recording arm we place the LCD sandwiched between two polarizers (P), which are oriented with the appropriate angles (45° for the first one and −45° for the last one) to produce amplitude-mostly modulation with a contrast of 20. Then, a 4F system is used to image the intensity transparency displayed on the reflective LCD onto the recording material. In previous works a transmissive LCD was used [19]. To generate the diffractive lenses, we use an LCoS-Pluto provided by Holoeye with a resolution of 1920x1080 (HDTV) pixels and a pixel size of 7.7x7.7 μm^2, previously characterized [20]. The analyzing arm is designed so that the beam of light incident onto the recording material is collimated. D1, a diaphragm, is used to limit the aperture of the collimated beam. We need to introduce a non-polarizing beam-splitter to make that both beams of light, the recording and the analyzing, follow the same path. After the recording material, we have introduced a red filter so that the light incident onto the final CCD camera is only coming from the analyzing beam. The lens recorded on the photopolymer is responsible for the focusing of the 633 nm wavelength beam. We image the point spread function (PSF) generated by the diffractive lens onto the CCD camera. We can

#251920 Received 14 Oct 2015; revised 11 Dec 2015; accepted 17 Dec 2015; published 20 Jan 2016

control the magnification of our experimental set-up using a 4-F system by the focal lengths of L3 and L4 [7]. We use a high dynamic range CCD, which is necessary to appreciate details in the PSF. This CCD camera model is pco.1600 from pco.imaging. A high dynamic 14 bits cooled CCD camera system with a resolution of 1600x1200 pixels and a pixel size of 7.4x7.4 μm^2. The camera is also used on the plane of the recording material to evaluate the intensity pattern actually imaged from the LCoS plane.

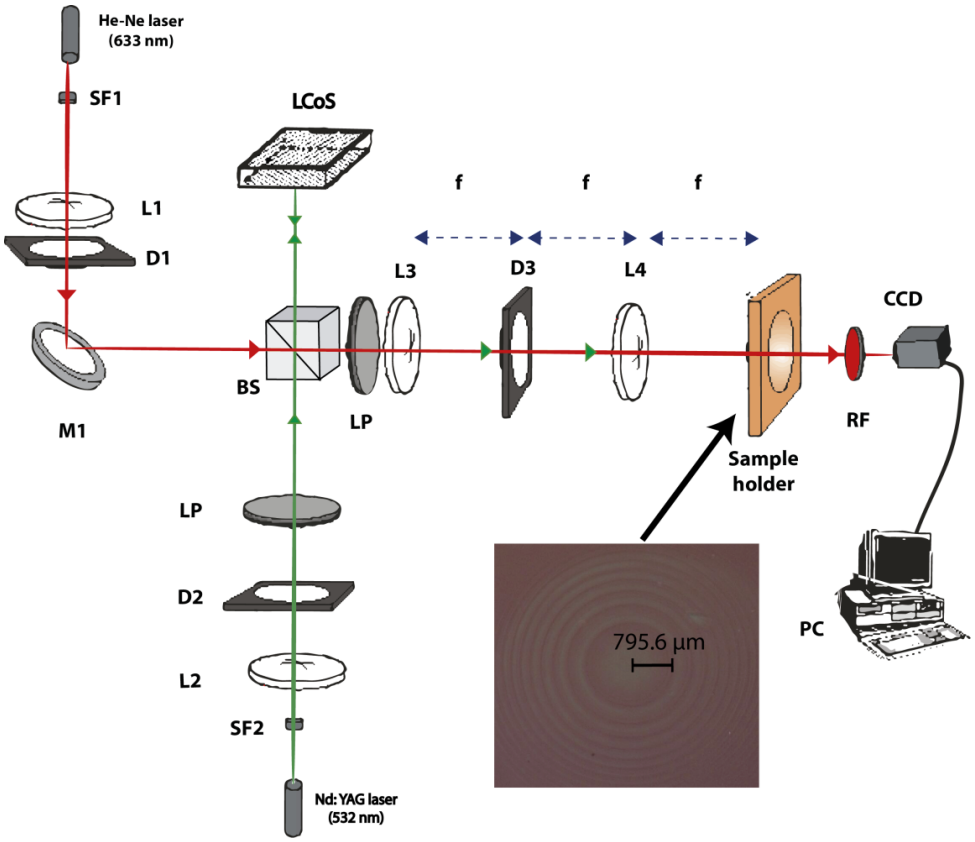

Fig. 2. Experimental setup used to register and analyze in real-time the DOEs (diffractive lenses) D, diaphragm, L, lens, BS, Beam splitter, SF, spatial filter, LP, lineal polarizer, RF, red filter.

In Fig. 3(a), we show the image obtained using the CCD camera when located in the recording plane. We see the characteristic ring structure with decreasing period as we move away from the center of the diffractive lens. In Fig. 3(b), we show the intensity plot along the horizontal line passing through the center of the lens. This intensity pattern in Fig. 3 is the exposure pattern that will be recorded on the photopolymeric material. It is important to note the high improvement in these images in comparison with the ones presented in [20], where the size of the pixels was larger, 44 µm, with the transmissive LCD. Therefore, intensity pattern was far from the ideal one, this differences are more accused in the boundaries of the lens where the distance between two consecutive peaks are smaller, as it can be seen in Fig. 1 where the ideal light distribution is depicted. This new spatial light modulation is composed by square pixel of 7.7 μm^2 that provides the opportunity of recording symmetric and asymmetric holographic patterns using a single beam [7] or alternative diffractive optical elements with more resolution.

#251920 Received 14 Oct 2015; revised 11 Dec 2015; accepted 17 Dec 2015; published 20 Jan 2016

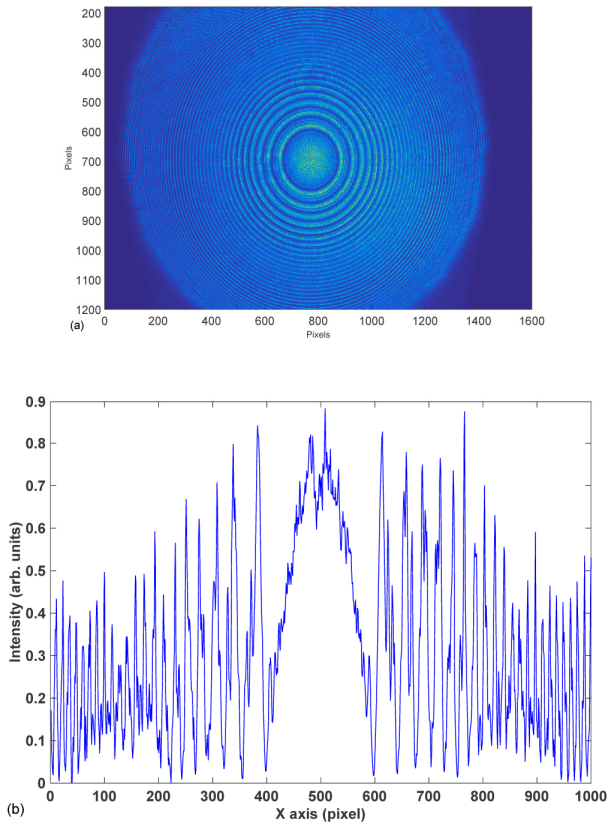

Fig. 3. (a) Image of the LCoS at the material plane (where the intensity transmittance equivalent lens is displayed) captured by the CCD camera. This plane is where the photopolymer should be placed. (b) Intensity profile across the horizontal line passing through the center of the lens.

In this work we use a photopolymer composed by acrylamide (AA) as polymerizable monomer, N,N'-methylene-bis-acrylamide (BMA) as crosslinking monomer, triethanolamine (TEA) as coinitiator and plasticizer, yellowish eosin (YE) as dye, polyvinyl alcohol (PVA) as binder and a small proportion of water as additional plasticizer. Different types of PVA can be used as a binder. In this work we have used a PVA 18-88 with Mw = 180000 amu. The particular concentration used in this work is presented in Table 1. To index match the photopolymer we used a glycerin with refractive index, n = 1.478. This value fits perfectly with our pre-exposed photopolymer with a refractive index of 1.477, measured with a refractometer and published in previous works [24].

For the preparation of the layer 30 ml of solution with water as the solvent is deposited using the force of gravity on a glass substrate (25 cm x 20 cm) and left in the dark (RH = 40–45%, T = 20–23 °C). When part of the water has evaporated (after about 36 hours), the layer has enough mechanical resistance and can be cut without deforming. The final "solid" film has a physical thickness around 90 ± 5 µm. This final thickness can be modified changing the quantity of the syrup deposited on the glass.

Table 1. Composition of the liquid solution for photopolymer AA.

TEA (ml)	PVA (ml) (8% w/v)	AA (gr)	BMA (gr)	YE (0.8% w/v) (ml)
2.0	25	0.84	0.2	0.6

#251920 Received 14 Oct 2015; revised 11 Dec 2015; accepted 17 Dec 2015; published 20 Jan 2016

4. Results and discussion

Once we control the beam shape projected onto photopolymer we want to analyze the influence of the material properties on the DOE recording. In this part, we present some of the results obtained with our model to simulate diffractive lenses in order to analyze the influence of each parameter on the final DOE and obtain an optimum energetic sensitivity and the maximum light intensity in the focal point. To analyze quantitatively the behavior of the lenses influenced by each specific parameter, we study the Fresnel propagation and the focus plane for each case. Firstly, we have estimated the viability of this material for diffractive lenses recording using the diffusion model. On the second place, once we have simulated the recording process introducing the specific parameters for this photopolymer into the model, we compare the experimental results with the theoretical prediction. When the model has been experimentally validated, we have explored the usefulness of the model to analyze the influence of each parameter on the lenses fabrication.

4.1. Recording diffractive lens onto photopolymer simulation

Our goal is to produce and simulate diffractive lenses, cylindrical and spherical, on the photopolymer with different focal lengths. To achieve this goal, we calculate the corresponding amplitude pattern to be displayed onto the LCD. There are two possibilities to store the optimum phase profile in our material. The first possibility, the diffractive lens can be directly projected onto recording material. To be more accurate, the second possibility, we can use the calibration obtained from the zero spatial frequency measurements [20], thus we can obtain the proper look-up table for the gray levels to be addressed onto the LCD. Here, what we display is an intensity transparency mask with the corresponding ring spacings for a diffractive lens of the desired focal length [20]. In this work, we have used the first method attending to the good focalizations obtained for the fabricated lenses, in this sense the linearity exhibited by this photopolymer at zero spatial frequency limit for the range of intensities between 0.05 mW/cm^2 and 2 mW/cm^2 and between 5 and 200 s of exposure [23] indicates that the first possibility can be applied for PVA/AA photopolymers.

In order to simulate the recording of the lenses in the photopolymer, the values of the main parameters are obtained from interferometric and diffractive techniques [23]. In this work these parameters are: $k_R = 0.007\ cm^2/(s \times mW)$, $\alpha = 0.02 \mu m^{-1}$, M_0 (volume fraction) = 0.22, $I_0 = 0.5 mW/cm^2$, γ (relationship between intensity and polymerization rate) = 0.93 and $D_0 = 3 * 10^{-10}\ cm^2/s$. In addition we have simulated alternative values D_0, α or γ keeping the rest of parameters constant to study the influence of each parameter in the fabrication of the lenses in other alternative photopolymers.

We have used the diffusion model to simulate the refractive index distribution generated by the incident beam modulated by the LCD. Once we have calculated the refractive index evolution in the illuminated zone, then we can obtain the instantaneous phase profile, $\varphi(x,y,t)$, which is introduced on the incident collimated beam. Since we consider the generated phase lens as a thin element the output electric field after the photopolymer is $\varphi(x,y)$. Then, we apply the Fresnel propagation [24] to calculate the intensity distribution with time at a distance of 1 meter. Therefore, we can numerically observe how during recording the light begins to focalize at this plane. These simulations are presented in Visualization 1, that is a simulation of the refractive index modulation distribution in the fabrication of the spherical lenses as function of time for the monomer diffusion of $D_0 = 3 * 10\text{-}10\ cm^2/s$ and Visualization 2, the simulated transverse cut of the focal plane. It is important to remark that due to the characteristics of the simulated photopolymer [9], we have designed chemically our material to obtain phase depth saturation slightly higher than 2π for a physical thickness of 95 ± 5 μm. When the recording time exceeds the optimum value of recording time, 120 s, the depth of the refractive index distribution generated exceeds the value of 2π and appears a degradation of the focalization: it overcomes the value of 2π. We have also simulated

#251920 Received 14 Oct 2015; revised 11 Dec 2015; accepted 17 Dec 2015; published 20 Jan 2016

cylindrical and spherical lenses with same values and we have not observed any significant difference. In order to obtain deeper insight into the quality of the simulated diffractive lenses, we have presented the transverse intensity distribution at focal plane in Fig. 4(a). In this Fig. 4(a), it can be seen as the model predicts a good focalization power of the lenses using our polymer parameters. In particular, in Fig. 4(b) we can see also the similarity of the desired refractive index distribution along the horizontal axis due to the high linearity of the material with this recording intensity and the low values of the monomer diffusion for the spatial frequencies range for this application. In Fig. 4(c) we show the intensity in the middle of the optical axis as a function of the distance, as it can be seen the focal length of this lens is 1 m as we expect.

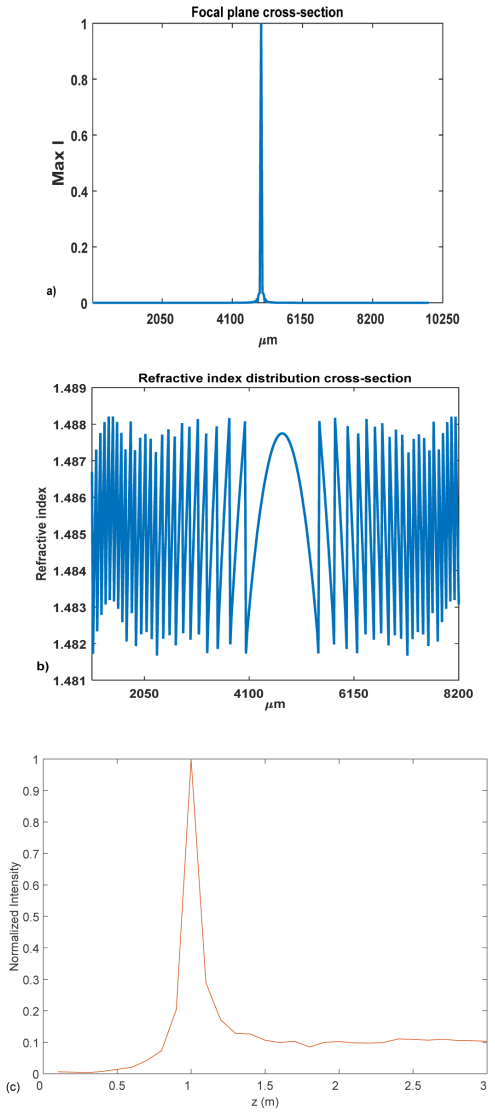

Fig. 4. Recording simulation for standard material for 120 s, optimum recording time. a) Transverse cut at the focal plane. Visualization 1 b) Transverse cut of the average refractive index distribution. Visualization 2 c) Axial cut of the focal plane, along light propagation. D = $3*10^{-10}$ cm^2/s. f = 1m.

#251920 Received 14 Oct 2015; revised 11 Dec 2015; accepted 17 Dec 2015; published 20 Jan 2016

4.2. Experimental diffusion model validation

Now it is time to check the simulations provided by the diffusion model with the experimental behavior proposed for the PVA/AA photopolymer. In Visualization 3 and Visualization 4, we present the temporal evolution during recording along the vertical transverse cut at the focal plane during the fabrication of a diffractive lens with 0.5m of focal length, spherical and cylindrical respectively. As it can be seen, the intensity begins to concentrate in the focal point and, after 120 s, it seems more or less similar, that means, in both cases the optimum recording time is the same as it can be expected. To quantify the energy, we present in Fig. 5 the normalized intensity in the focal point for the recording of a spherical lens with a 0.5 m focal length, as a function of time. Here it is demonstrated the good agreement between the diffusion model and the experiments, together with the high focalization power of the diffractive lenses. That opens an interesting way to produce cheap and manageable diffractive lenses using PVA/AA photopolymer. We have measured the focus length, obtaining a value of 500 ± 1 mm as we expected. Also, the model predicts the optimum recording time for these lenses and the decrease of the focal point intensity when the exposure time is longer than the optimum and the phase modulation overcomes the value of 2π.

Now let us quantify the importance of different parameters in the fabrication of the diffractive lenses. In Fig. 6 we show the simulated behavior of the photopolymer for different focal lengths, 0.5, 1 and 2 m respectively for a 95 μm of layer thickness. In all the cases after the optimum recording time when the maximum focal power is achieved, the intensity in the focal point starts to decrease due to the overmodulation of the refractive index. It is also important to notice that the simulated behavior exhibited by the photopolymer in the recording of spherical and cylindrical lenses with different focal lengths is similar. In Fig. 6(a) we show the simulations obtained using the model for the different focal distances and for a 95 μm of layer thickness. In addition, as it is shown in Fig. 6(b) experimentally the spherical lenses of 0.5 and 1 m also present similar behavior for both focal length, in this case the layer thickness was 85 μm. This can be explained by the relatively low influence of monomer diffusion for this long spatial periods provided by the spatial light modulator, and the polymerization has stronger influence than diffusion on the phase image formation. Comparing Fig. 6(a) to Fig. 6(b) we show as the model can predict the behavior for different thicknesses and the optimum focalization power is achieved with longer exposition for thinner materials.

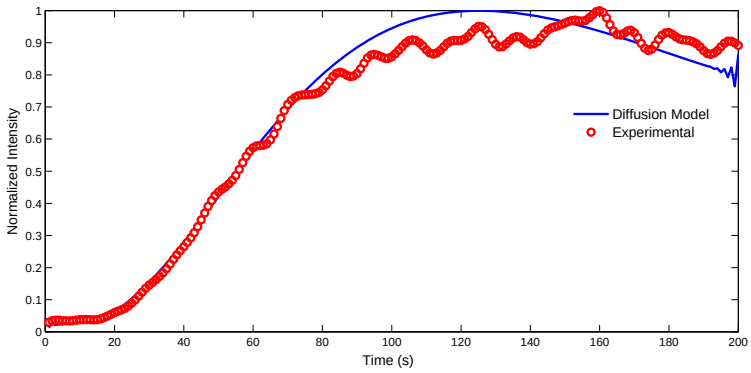

Fig. 5. Intensity at the focal point as a function of the experimental recording and the theoretical simulation for spherical lens f = 0.5 and layer thickness of 95 ± 2 μm. Visualization 3 and Visualization 4.

#251920 Received 14 Oct 2015; revised 11 Dec 2015; accepted 17 Dec 2015; published 20 Jan 2016

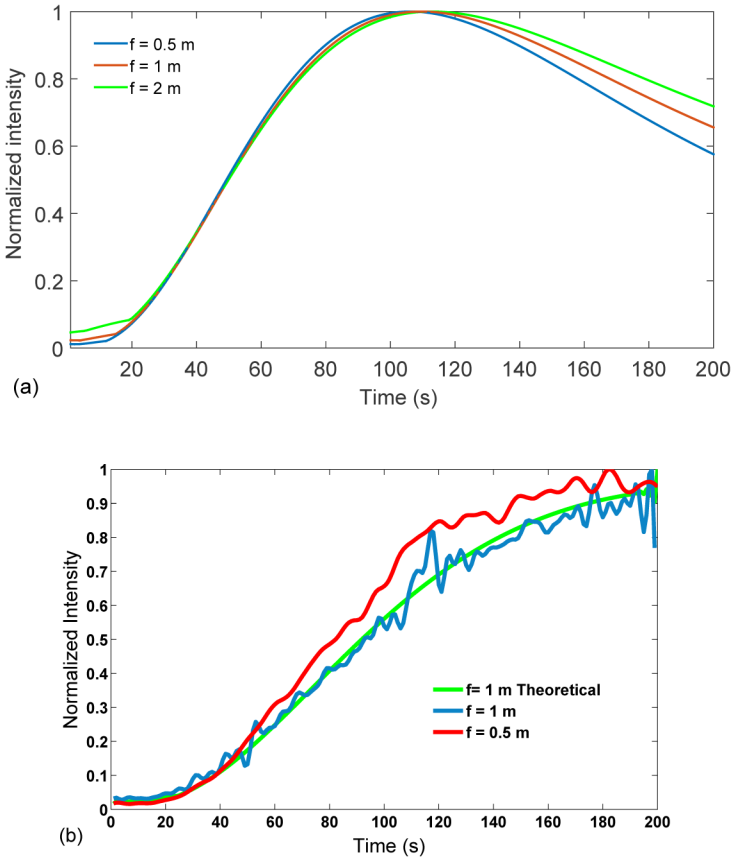

Fig. 6. Intensity at the focal point as a function of recording time for different focal length (2, 1, and 0.5). a) Simulation provided by diffusion model. b) Experimental results with thickness and 85 ± 2 μm and for f = 0.5 m and f = 1m.

4.3. Influence of the material parameters on the diffractive lens

Now we will study the influence of D_0, α and γ parameters on the refractive index distribution stored. We study the variation of one of these parameters and keep the rest constant. It is important to notice that in previous works [22] we have studied the influence of the non-local polymerization introduced by Sheridan et al. [14]. In the non-local-polymerization model, the square root of σ is related to the polymer chain length, and we demonstrated in [21] that for the very low spatial frequencies the size of the polymer length does not affect the refractive index distribution. Therefore it can be assumed that the polymerization process is local, thus σ = 0.

To check the influence of the D_0 parameter, we have simulated different lenses with a range of values of diffusion and verify how the diffusion influences in the focal plane. In particular, we obtain optimum recording time to achieve the maximum intensity at the focal point. We study the influence of the monomer diffusion in the formation of the diffractive optical lens and the results are plotted in Fig. 7. We have simulated the intensity in the focal point for the values of D_0 of $3\cdot10^{-8}$ cm^2/s, $3\cdot10^{-9}$ cm^2/s, $3\cdot 10^{-10}$ cm^2/s and $3\cdot10^{-11}$ cm^2/s. We do not observe important differences for the two smallest values of monomer diffusion. In opposition, we appreciate clearly a significant variation for the two highest value of monomer diffusion. That means that the increase of the monomer diffusion have influence for these spatial frequencies when it takes a value higher than $3\cdot10^{-10}$ cm^2/s. Below this value, its influence is relatively low in the diffractive lens formation. It is important to remark the low

#251920 Received 14 Oct 2015; revised 11 Dec 2015; accepted 17 Dec 2015; published 20 Jan 2016

intensity values achieved at the focal point when the diffusion is high: this is due to the smoothing of the sharp phase profile, in particular in the transitions between maximum and zero values, and shown in Fig. 1.

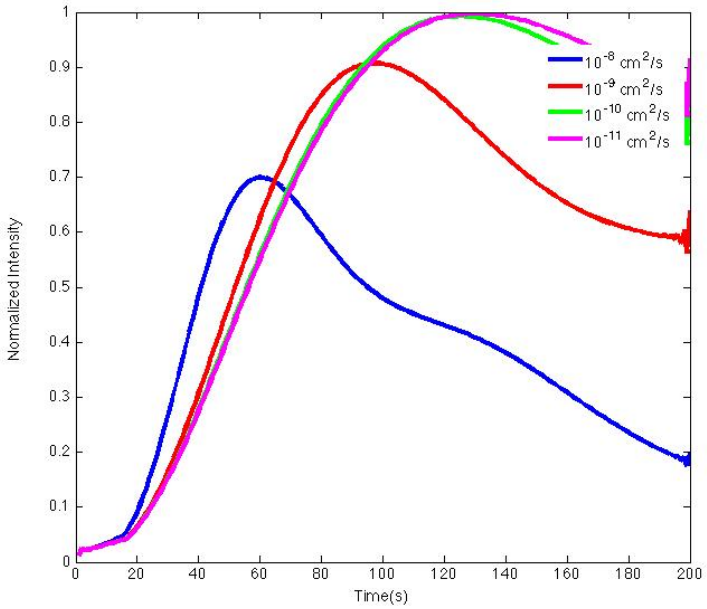

Fig. 7. Intensity of the focal spot as a function of recording time for different internal monomer diffusivities.

Let us now study the influence of the relationship between intensity and polymerization rate parameter (γ) with the diffusion model. This parameter, γ, represents the non-linearity of the polymerization with the incident light into the material, in principle close to 0.5 for less viscous polymerizable systems and close to 1 for more viscous ones, like PVA/AA materials. We have simulated a cylindrical and a spherical lens with the parameters used along this paper, D_0 of 10^{-10} cm^2/s and 200 s of continuous exposition. As we have said above, γ is directly related to the linearity in the material response and, in this case, any change in this parameter affects to the refractive index distribution stored in the photopolymer. In opposition to what we expect, a variation in this parameter only affects slightly to the focalization power of the lenses recorded, that is good news for more liquid polymeric systems that can be used also to record diffractive lenses.

#251920 Received 14 Oct 2015; revised 11 Dec 2015; accepted 17 Dec 2015; published 20 Jan 2016

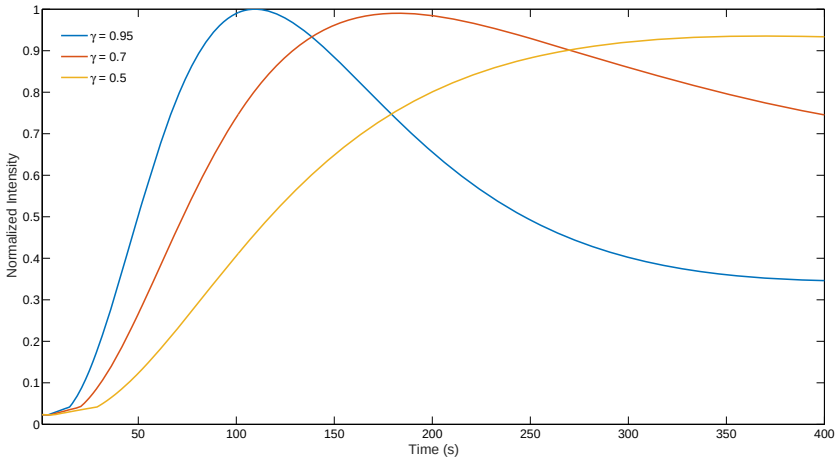

Fig. 8. Intensity of the focal point as a function of recording time for different internal relations between intensity and polymerization.

Next, we are going to show the influence of the variations of the depth attenuation. To study this case, we have simulated lenses with the same parameters as in the previous section during 200 s of recording and a D_0 value of 3.10^{-10} cm^2/s (Fig. 8). The simulations have been done for five values of α: 2 nm^{-1} 10 nm^{-1}, 20 nm^{-1}, 40 nm^{-1}, and 60 nm^{-1}. The results are presented in Fig. 9. As we expect the variation of this parameter just influences the velocity of focalization, due the variation of the effective optical thickness of the layer.

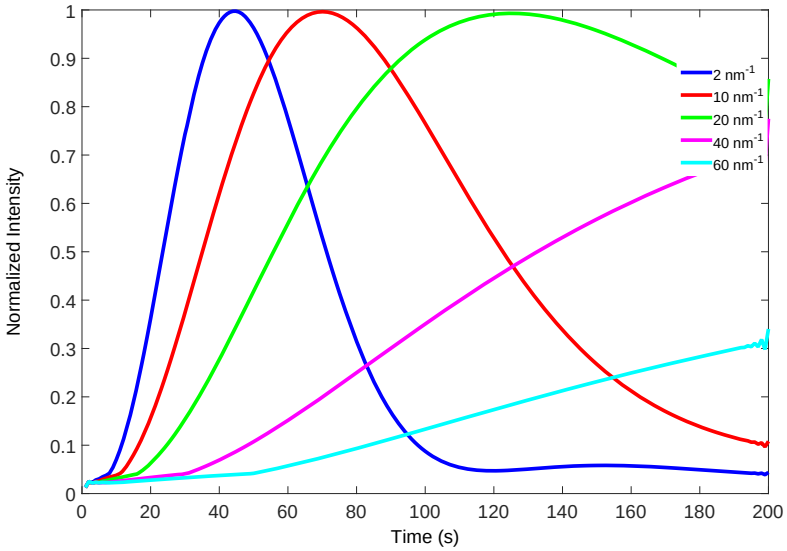

Fig. 9. Intensity at the focal point as a function of recording time for different internal dye absorption.

To finish this section we have analyzed the variation also in np and K_R, and both only have influence in the time required to achieve the best focal point like the behavior shown in Fig. 9, but not on the focalization power of the lens. For example, the optimum recording time

#251920 Received 14 Oct 2015; revised 11 Dec 2015; accepted 17 Dec 2015; published 20 Jan 2016

decreases when these polymerization constant, K_R, is increased as can be deduced from the model Eqs. easily.

5. Conclusions

Along this work, we have analyzed the influence of the material properties, diffusion rates, absorption, and linearity on the lenses recording during the recording of cylindrical and spherical lenses in photopolymers. We have validated the model to reproduce and predict the experimental behavior of the photopolymer in the lenses fabrication. We have detected the decay in the focalization power in the recorded lenses when the diffusion rate is high. In this sense, we have shown that recording diffusion rates lower than 10-10 cm2/s are required. Next, we have demonstrated that attenuations higher than 0.02 μm-1 for layers 100 μm thick can improve the recording of the lenses due to the increase of the effective optical thickness. Furthermore, we have demonstrated the importance of the relation between intensity and polymerization, showing as the more liquid photopolymeric system can be used also to record diffractive lenses. To summarize we presented a practical and elastic method to fabricate and simulate diffractive lenses in photopolymers. Taking into account the results presented, for the optimal fabrication of a particular lens we should choose a particular photopolymer with the desired parameters and then design the better intensity distribution to record it.

Acknowledgments

This work was supported by the "Ministerio de Economía y Competitividad" (projects FIS2011-29803-C02-01, FIS2011-29803-C02-02 and FIS2014-56100-C2-1-P) and by the "Generalitat Valenciana" of Spain (projects PROMETEOII/2015/015 and ISIC/2012/013).

#251920 Received 14 Oct 2015; revised 11 Dec 2015; accepted 17 Dec 2015; published 20 Jan 2016